Journal of Solid State Chemistry **159,** 134–138 (2001)
doi:10.1006/jssc.2001.9141, available online at http://www.idealibrary.com on IDEAL®

Extraordinarily Short Pb–Pb Bonds in the New Binary Intermetallic $Ti_6Pb_{4.8}$

Holger Kleinke

Department of Chemistry, University of Waterloo, Waterloo, Ontario, Canada N2L 3G1

Received December 16, 2000; in revised form February 14, 2001; accepted March 5, 2001; published online April 27, 2001

$Ti_6Pb_{4.8}$ is accessible via reactions in a Pb flux starting from the elements in evacuated silica tubes at 680°C. Larger single crystals can be obtained by adding traces of iodine to promote crystal growth. At higher temperatures, $Ti_6Pb_{4.8}$ decomposes into Ti_4Pb and Pb. $Ti_6Pb_{4.8}$ crystallizes in the hexagonal α-Ti_6Sn_5 type, space group $P6_3/mmc$, with the lattice dimensions $a = 939.23(8)$ and $c = 579.01(5)$ pm for $Ti_6Pb_{4.824(7)}$ ($Z = 2$). While the structure is dominated by the heteronuclear Ti–Pb bonds, linear Ti and Pb chains run parallel to the c axis with interatomic distances being equidistant by symmetry $c/2 = 289.5$ pm). This results in a Pb–Pb distance being much shorter than a Pb–Pb single bond (typically 310 pm). Longer homonuclear distances of about 315 pm (Ti–Ti) and between 357 and 374 pm (Pb–Pb) occur perpendicular to the chain direction. All these interactions have bonding character, as the LMTO calculations of $Ti_6Pb_{4.8}$ reveal. © 2001 Academic Press

Key Words: **intermetallics; titanium plumbide; structure and bonding; electronic structure; hypervalent bonding.**

INTRODUCTION

For several decades, different research and industrial groups have been using high-temperature flux methods that use different melts of elements (or, e.g., oxides and salts like LiCl/KCl) to get large, high-quality crystals (1). Some suitable elements are found among the main groups, e.g., aluminum (2), tin (3), antimony (4), and bismuth (5), while the transition metals are less propagated because of their higher melting points. Rare exceptions include the use of chromium and iron for the crystal growth of Zr_2S (6) and H_7P_4 (7), respectively.

Ideally, good flux materials occur in the molten state over a wide temperature range. They should be highly unreactive toward the crystals to be prepared, unless their constituent elements are also part of the desired products. It is furthermore advantageous when the flux can easily be removed, such as tin with weak acids. Therefore, tin has been used as the flux for the crystallization of a multitude of different phosphides at different temperatures in the group of Jeitschko. However, adding tin in syntheses aiming at early transition metal antimonides would cause inherent problems due to possible tin/antimony mixing, which would be difficult to examine with X-ray investigations because of the comparable scattering factors of the Sn and Sb atoms.

Focusing on lead instead of tin, it is exciting to realize that lead is most unwilling to form compounds with antimony or early transition metal atoms—especially when being interested in early transition metal antimonides (8). The only known group 4 plumbides are Ti_4Pb (9), Zr_5Pb and Zr_5Pb_{4-x} (10), and Zr_5Pb_3 (11). In order to further explore especially the Pb-rich part of these systems, various experiments were performed, the results of which proved the existence of at least one more titanium plumbide, namely $Ti_6Pb_{4.8}$, which is the most Pb-rich compound in the Ti/Pb system under the reactions conditions applied. This article will tackle the synthesis and crystal and electronic structure of $Ti_6Pb_{4.8}$.

EXPERIMENTAL

Synthesis

$Ti_6Pb_{4.8}$ readily forms at elevated temperatures (680°C) from the elements in a 1:1 ratio in an evacuated fused silica tube. The small excess of elemental lead remains unreacted. Starting from Pb-deficient Ti:Pb ratios, e.g., 3:2, gave the same main product, i.e., $Ti_6Pb_{4.8}$. $Ti_6Pb_{4.8}$ decomposes upon annealing at 1300°C under inert atmosphere into Ti_4Pb and Pb. This is assumed to be the main reason for this compound to stay concealed until today (in analogy to the recently uncovered most Sn-rich Ti stannide Ti_2Sn_3 (12), but in contrast to Ti_6Sn_5 (13) which melts congruently at 1490°C (14)). Better crystals of $Ti_6Pb_{4.8}$ can be obtained by annealing a mixture of the elements in a 1:1 ratio at 600°C under addition of traces of iodine as a mineralizator. EDX investigation carried out on selected crystals revealed the existence of solely Ti and Pb, in the ratio of 52(3):48. For comparison: the refined composition $Ti_6Pb_{4.8}$ corresponds to 55.6:44.4, thus the EDX investigations suggest a slightly smaller Ti content.

0022-4596/01 $35.00

Structure Determination

A single crystal data collection was performed using a diffractometer with an area detector. The data were corrected for Lorentz and polarization effects. The space group of the α-Ti_6Sn_5 type, $P6_3/mmc$, is consistent with the systematic extinctions observed experimentally ($l = 2n + 1$ for all *hhl* reflections). The structure refinement in the centrosymmetric space group was successful (program SHELXL (15)). The high displacement parameter U_{eq} of Pb1 pointed toward a not completely filled position. Refinement of the occupancy factor f(Pb1) yielded $f = 0.824(7)$ by lowering the residual factor $R(F_o)$ from 0.0327 to 0.0217; it still gave a high U_{eq} of Pb1 due to enlarged vibrations along the *c* axis, as reflected in U_{33}, which corresponds to almost 10 times U_{11} ($U_{11} = U_{22}$ by symmetry).

In this structure model, Pb1 occupies the site 2*a*, i.e., (0, 0, 0) and (0, 0, $\frac{1}{2}$), forming a linear chain with equidistant Pb1–Pb1 distances of $c/2 = 289.5$ pm. Refinements of split positions or in lower symmetry space groups failed: attempts were made in $P6_3mc$, a direct subgroup of $P6_3/mmc$, wherein the Pb1 atom would be on the still symmetry equivalent positions (0, 0, *z*) and (0, 0, $z + \frac{1}{2}$), and in $P3m1$, a direct subgroup of $P6_3mc$, wherein Pb1 would be located on two nonequivalent positions (0, 0, *z*) and (0, 0, *z*′). The latter would enable a distortion in the linear Pb1 chain running parallel to [001]. However, no differences between the two Pb1 positions in $P3m1$ were found; within the standard deviations, they were refined to be on (0, 0, 0) and (0, 0, $\frac{1}{2}$). Allowing Pb1 to move away from $x = 0$ and $y = 0$ neither improved nor changed the structure model. Also, no superstructure reflections were found using longer exposure times with the area detector (three minutes per frame). However, mixed Ti/Pb occupancies cannot be ruled out, but they are rather unlikely because of the character and size differences between Ti and Pb atoms. Also, that could not explain the high anisotropy of the thermal parameter. Such a refinement led to a refined stoichiometry of "$Ti_{6.23}Pb_{4.77(1)}$," a Ti:Pb ratio of 56.6:43.4, contradicting the EDX results.

Since $Ti_6Pb_{4.824(7)}$ formed in equilibrium with unreacted lead, it represents the upper limit of Pb occupancy of this position. No shifts in the lattice parameters were observed by going to Ti-rich starting compositions (e.g., Ti:Pb = 3:2). It is concluded that $Ti_6Pb_{4.8}$ exhibits no significant phase range. Crystallographic details may be found in Table 1. Atomic positions, equivalent displacement parameters, and occupancy factors are given in Table 2.

Electronic Structure Calculations

Calculations were carried out using the LMTO approach on Ti_6Pb_5, assuming full occupancies of all positions. Within the self-consistent TB-LMTO-ASA program (TB-LMTO-ASA: tight binding linear muffin tin orbitals atomic spheres approximation) (16, 17), the density functional theory (18) is used with the local density approximation (LDA). The ASA radii were determined to be 1.624 (Ti1), 1.623 (Ti2), 1.672 (Pb1), 1.693 (Pb2), and 1.694 pm (Pb3). The integration in *k* space was performed by an improved tetrahedron method (19) on a grid of 549 irreducible *k* points in the irreducible section of the first Brillouin zone.

TABLE 1
Crystallographic Data for $Ti_6Pb_{4.8}$

Chemical formula: $Ti_6Pb_{4.824(7)}$	Space group: $P6_3/mmc$ (No. 194)
Formula weight: 1287.1 g/mol	Crystal size [mm]: $0.10 \times 0.08 \times 0.06$
$a = 939.23(8)$ pm	$T = 22°C$
$c = 579.01(5)$ pm	$\lambda = 71.069$ pm
$V = 442.34(7)\ 10^6 pm^3$	2θ range: 5.0–60.7°
$Z = 2$	$\rho_{calcd} = 9.66\ g/cm^3$
Collected reflections: 4342	Independent reflections: 286 ($R_{int} = 0.086$)
Observed reflections/parameter: 255/19	Extinction coefficient: 0.0128(6)
Absorption correction: numerical	$T_{min} = 0.0068$, $T_{max} = 0.0537$
$\mu = 964.5\ cm^{-1}$	$R(F_o)^a = 0.022$; $R_w(F_o^2)^b = 0.047$

$^a R(F_o) = \sum \|F_o| - |F_c\| / \sum |F_o|$.
$^b R_w(F_o^2) = [\sum [w(F_o^2 - F_c^2)^2] / \sum [w(F_o^2)^2]]^{1/2}$.

RESULTS AND DISCUSSION

Crystal Structure

$Ti_6Pb_{4.8}$ crystallizes in the hexagonal α-Ti_6Sn_5 type. While the hexagonal α-Ti_6Sn_5 was originally reported to be the high-temperature modification (13), the existence of the low-temperature orthorhombic variant could not be confirmed in a recent reinvestigation of the Ti/Sn phase diagram (14). During our studies on $Ti_6Pb_{4.8}$ we found no evidence for a low-temperature modification in the Ti/Pb system, either.

In addition to $Ti_6Pb_{4.8}$ and α-Ti_6Sn_5, only a few gallides are known to form this type, namely $Ti_{2.5}Mn_{2.95}Ga_{4.55}$ (20), $Mn_{5.4}Cu_{0.6}Ga_5$ (21), $(V_{1-x}Nb_x)_6Ga_5$ ($0 \le x \le 0.55$) (22), and Ta_6Ga_5 (high-pressure phase) (23). Only powder X-ray data were reported in all of these cases.

TABLE 2
Atomic Positions, Equivalent Displacement Parameters, and Occupancy Factors of $Ti_6Pb_{4.8}$

Atom	site	*x*	*y*	*z*	U_{eq}/pm^2	*f*
Ti1	6*g*	$\frac{1}{2}$	0	0	43(4)	1
Ti2	6*h*	0.1568(2)	0.3137	$\frac{3}{4}$	66(5)	1
Pb1	2*a*	0	0	0	138(4)	0.824(7)
Pb2	2*d*	$\frac{1}{3}$	$\frac{2}{3}$	$\frac{3}{4}$	37(2)	1
Pb3	6*h*	0.20068(3)	0.79932	$\frac{1}{4}$	50(2)	1

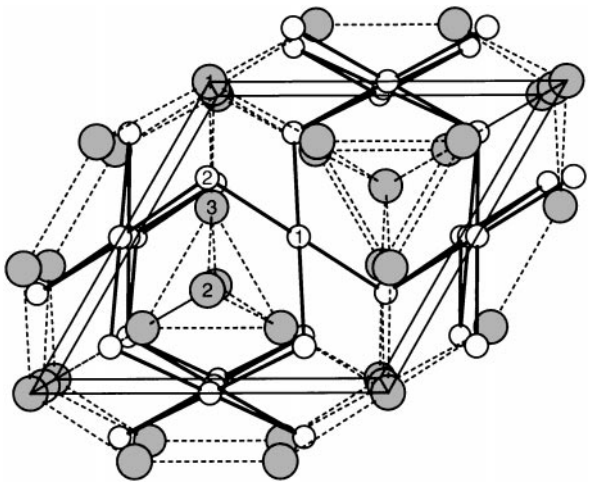

FIG. 1. Structure of $Ti_6Pb_{4.8}$ in a projection along [001]. (Small, white circles) Ti; (large, gray circles) Pb. Only Ti–Ti and Pb–Pb bonds are shown.

The projection of $Ti_6Pb_{4.8}$ along the hexagonal *c* axis is shown in Fig. 1, emphasizing the homonuclear interactions. The structure of $Ti_6Pb_{4.8}$ can be described based on the homonuclear interactions as follows. The Pb1 atoms, forming linear chains along the *c* axis, are surrounded by six chains of trigonal Pb2-centered $Pb3_6$ prisms. All of these interactions are presumably weak with distances between 357 and 374 pm (dashed lines in Fig. 1), except for the short Pb1–Pb1 bond within the linear chain of 289.5 pm. Interwoven with the Pb network is a Ti network with interatomic distances of 289.5 pm in the linear Ti1 chain, running parallel to [001], and of 315 pm for the Ti1–Ti2 interactions (solid lines in Fig. 1). (see Table 3.)

Alternatively, the structure can be regarded as an intergrowth of $Ti1Pb_6$ octahedra, which are face-condensed to linear chains parallel to [001], and bi-capped $Ti2Pb_5$ pentagons, which are edge-condensed to form chains parallel to [001]. The two Pb caps of every single $Ti2Pb_5$ pentagon are also part of the next pentagons. Four Ti1 neighbors in distances of 315 pm complete the Ti2 surrounding to a polyhedron with 11 corners. Therein, the Ti2 atom is situated between a Pb_4 ring and a Pb-capped Ti_4Pb_2 ring. Including the surrounding Ti2 atoms within 315 pm, the Ti1 atom is located in the center of a (distorted) Ti_6Pb_6 icosahedron, which can be viewed as two interwoven Ti_6 and Pb_6 octahedra. The coordination spheres of all five symmetry inequivalent atom sites are highlighted in Fig. 2.

TABLE 3
Selected Interatomic Distances of $Ti_6Pb_{4.8}$

Ti1–Pb3	287.27(3)	4×	Ti2–Pb2	287.1(2)	1×
–Ti1	289.51(3)	2×	–Pb1	293.4(2)	2×
–Pb2	307.40(2)	2×	–Pb3	297.3(2)	2×
–Ti2	314.7(2)	4×	–Pb3	298.16(6)	2×
			–Ti1	314.7(2)	4×
Pb1–Pb1	289.51(3)	2×	–Ti2	385.9(2)	4×
–Ti2	293.4(2)	6×			
–Pb3	357.12(4)	6×	Pb3–Ti1	287.27(3)	4×
			–Ti2	297.3(2)	2×
Pb2–Ti2	287.1(3)	3×	–Ti2	298.16(7)	2×
–Ti1	307.40(2)	6×	–Pb1	357.12(4)	2×
–Pb3	361.05(3)	6×	–Pb2	361.05(3)	2×
			–Pb3	373.78(5)	2×

Including all neighboring atoms up to a distance of 315 pm, the coordination numbers for the Pb atoms are eight for Pb1 (located in a Pb bi-capped Ti_6 octahedron), nine for Pb2 (a tri-capped trigonal prism comprising solely Ti atoms), and eight for Pb3 (a bi-capped trigonal prism, again consisting of Ti atoms only).

The heteronuclear interactions outweigh the homonuclear interactions by number and shortness. The Ti–Pb distances vary from 287 to 307 pm, which is slightly larger than the sum of the atomic radii of 282 pm (taken from Pauling's single bond radii: $r_{Ti} = 132$ pm; $r_{Pb} = 150$ pm (24)). The Ti–Ti contacts of 289.5 and 315 pm are inconspicuous as well. Elemental titanium crystallizes in the hexagonal closed packing (Mg type) with interatomic distances of 289 and 295 pm, and linear Ti–Ti chains with different interatomic separations were found in (Zr, Ti)Sb ($d = 284$ pm (25)), Ti_2Sn_3 ($d = 298$ pm (12)), and TiSb ($d = 315$ pm).

All of the Ti–Ti distances named above were calculated to be of bonding nature (12, 25). The character of the longer Pb–Pb interactions in $Ti_6Pb_{4.8}$ of 357–374 pm is questionable. These distances may be compared to the bonds in elemental lead (350 pm in the cubic face-centered packing), being much longer than typical Pb–Pb single bonds. Note that lead is more electronegative than titanium on any electronegativity scale; e.g., the Allred–Rochow electronegativities are 1.32 for Ti and 1.55 for Pb (Pauling, 1.54 vs 2.33). The Ti atoms therefore will reduce the Pb atoms to some extent, so that one should consider Pb–Pb single bonds of negatively charged Pb atoms. Examples may be found among the Zintl phases, including 310 pm in Pb_4^{4-} tetrahedra in KPb (26) and 313 pm in infinite zigzag Pb^{2-} chains in BaPb (27). These distances are considerably longer (by more than 7%) than the shortest Pb–Pb bond observed here (289.5 pm), which may be compared to the bond in the slightly deficient linear Pb chain in Zr_5Pb_{4-x} (10). Therein, the Pb–Pb distance increases with increasing Pb content, i.e., from 299.6 pm with a 87% Pb occupancy to 300.5 pm with a 94% Pb occupancy.

Band structure calculations of linear chains comprising late main group elements (like Sn, Pb, and Sb) have indicated the ideal electron count being seven electrons per atom, i.e., a bond order of $\frac{1}{2}$ (8, 25, 28, 29). It is concluded that the extraordinary shortness of the interatomic distances in the Pb chain in $Ti_6Pb_{4.8}$ (i.e., matrix effects) is responsible for the defects, reflected in the 82.4(7)% occupancy of

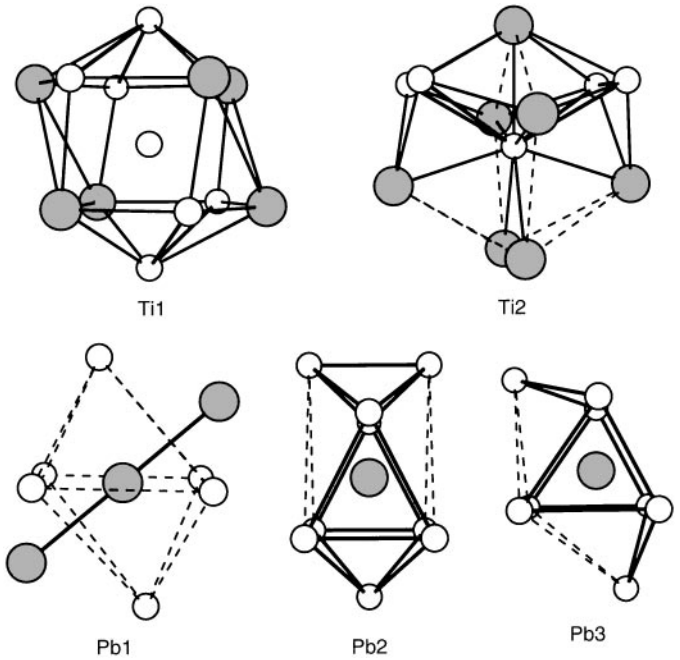

FIG. 2. Coordination spheres of the five crystallographically different atom sites. Central atoms, from top left to bottom right are: Ti1, Ti2, Pb1, Pb2, and Pb3.

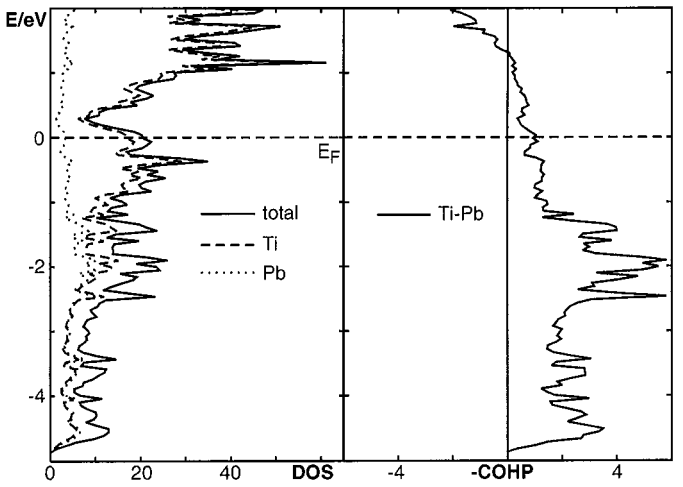

FIG. 3. (left) DOS curves of Ti_6Pb_5; (right) cumulated Ti–Pb COHP curves.

that Pb site (Pb1 in Table 2). Accordingly, the high displacement parameter along the chain direction U_{33}(Pb1) indicates the tendency of the Pb1 atoms shifting away from one another toward the voids, which does not lower the symmetry in the averaged structure as determined by the X-ray investigation. No anomalies are to be expected among the other representatives of the α-Ti_6Sn_5 type, for therein, the interatomic distances in the linear chains are not unusual because of the smaller sizes of the main group atoms Ga and Sn, respectively.

Electronic Structure

The calculated densities of states (DOS) and Ti–Pb crystal orbital Hamiltonian populations (COHP (30)), cumulated over all Ti–Pb bonds per unit cell, of the structure model Ti_6Pb_5 are shown in Fig. 3. The DOS curve is typical for metallic intermetallic compounds. A significant number of states are filled at the Fermi level E_F, which consist mainly of Ti-based orbitals. The contributions of the more electronegative main group element Pb to the conduction band are concentrated at lower energies, but still present at and above the Fermi level. The Ti contributions at these energies, i.e., below -3 eV, indicate covalent mixing. These general features are comparable to those of the densities of states of the stannides and antimonides (see, e.g., (8, 12, 25)).

Averaged over the first Brillouin zone, only bonding Ti–Pb interactions are filled up to the Fermi level. Raising the Fermi level, i.e., increasing the number of valence electrons, would further strengthen the Ti–Pb bonds by filling more bonding states. Note that bonding interactions exhibit negative COHP values by definition (30), in contrast to the crystal orbital overlap populations (COOPs (31)).

The COHPs of the cumulated homonuclear interactions are shown in Fig. 4. As for the Ti–Pb interactions, no antibonding Ti–Ti states occur below the Fermi level. The short Ti–Ti bond (289.5 pm) is almost twice as strong as the longer bond (315 pm), which is reflected in the integrated COHP values of -1.52 vs -0.87 eV per bond. Calculations of a structure model with equally short Ti–Ti distances reveal this being solely due to the different lengths, which come from optimized Ti–Pb bond lengths. However, as the

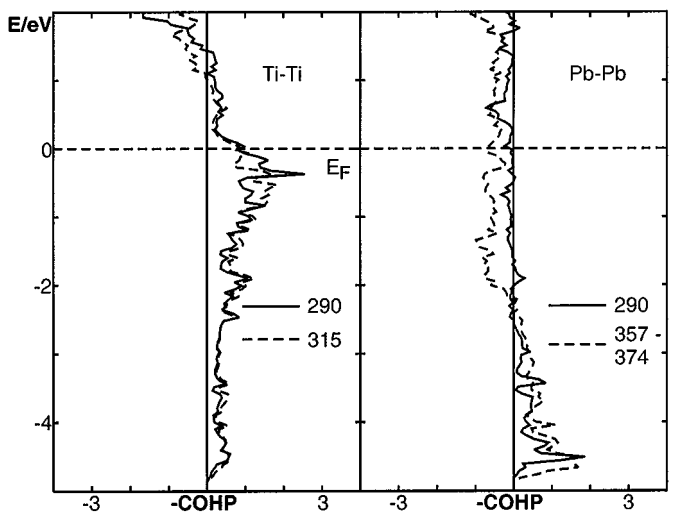

FIG. 4. (left) Cumulated Ti–Ti and (right) Pb–Pb COHP curves.

longer Ti–Ti bond occurs twice as often per unit cell, the two different Ti–Ti COHP curves are most similar after cumulating over the whole unit cell.

On the other hand, antibonding Pb–Pb states are filled starting at -2 eV. In the case of the short bond of 289.5 pm, the filled bonding states outweigh by far the antibonding states, whereas the ratio of filled bonding states to filled antibonding states is almost equal in the longer interactions (357–374 pm). Their integrated COHPs range from -0.10 to -0.06 eV, indicating weak bonding character, which is about 10% of the short bond (-1.04 eV).

SUMMARY

The new metallic compound $Ti_6Pb_{4.8}$ has been uncovered and structurally characterized. Its structure (α-Ti_6Sn_5 type) comprises—in addition to the dominating heteronuclear Ti–Pb bonds—bonding homonuclear interactions of both kind, namely Ti–Ti as well as Pb–Pb bonds. The most striking feature of the crystal structure is the presence of the parallel running equidistant linear Ti and Pb chains. The latter exhibits Pb–Pb bonds being shorter than a single bond, causing deficiencies and enlarged thermal parameters within the linear Pb chain.

ACKNOWLEDGMENT

Financial support from the Natural Sciences and Engineering Research Council of Canada is appreciated.

REFERENCES

1. D. Elwell, High-temperature Solution Growth, *in* "Crystal Growth" (B. R. Pamplin, Ed.), 2nd ed. Pergamon Press, Oxford, 1980, and references cited therein.
2. X. Z. Chen, S. Sportouch, B. Sieve, P. Brazis, C. R. Kannewurf, J. A. Cowen, R. Patschke, and M. G. Kanatzidis, *Chem. Mater.* **10,** 3202 (1998).
3. P. Kaiser and W. Jeitschko, *J. Solid State Chem.* **124,** 346 (1996).
4. K. D. Myers, S. L. Bud'ko, I. R. Fisher, Z. Islam, H. Kleinke, A. H. Lacerda, and P. C. Canfield, *J. Magn. Magn. Mater.* **205,** 27 (1999).
5. R. A. Logan and C. D. Thurmond, *J. Electrochem. Soc.* **119,** 1727 (1972).
6. X. Yao and H. F. Franzen, *J. Less-Common Met.* **142,** L27 (1988).
7. H. Kleinke and H. F. Franzen, *Angew. Chem. Int. Ed. Engl.* **35,** 1934 (1996).
8. H. Kleinke, *Chem. Soc. Rev.* **29,** 411 (2000).
9. H. Nowotny and J. Pesl, *Monatsh. Chem.* **82,** 344 (1951).
10. Y.-U. Kwon and J. D. Corbett, *J. Alloys Compd.* **190,** 219 (1993).
11. H. Nowotny and H. Schachner, *Monatsh. Chem.* **84,** 169 (1953).
12. H. Kleinke, M. Waldeck, and P. Gütlich, *Chem. Mater.* **12,** 2219 (2000).
13. J. H. N. van Vlucht, H. A. C. M. Bruning, H. C. Donkersloot, and A. H. Gomes de Mesquita, *Philips Res. Rep.* **19,** 407 (1964).
14. C. Kuper, W. Peng, A. Pisch, F. Goesmann, and R. Schmid-Fetzer, *Z. Metallk.* **89,** 855 (1998).
15. G. M. Sheldrick, "SHELXL-97." Universität Göttingen, Germany, 1997.
16. O. K. Andersen, *Phys. Rev. B* **12,** 3060 (1975).
17. H. L. Skriver, "The LMTO Method." Springer-Verlag, Berlin/New York, 1984.
18. U. van Barth and L. Hedin, *J. Phys. C* **4,** 2064 (1971).
19. P. E. Blöchl, O. Jepsen, and O. K. Andersen, *Phys. Rev. B* **49,** 16,223 (1994).
20. V. Y. Markiv and A. I. Skripta, *Russ. Metall.* 196 (1986).
21. V. Y. Markiv and N. N. Belyavina, *Russ. Metall.* 204 (1986).
22. F. S. Kreidenko, V. Y. Markiv, and E. M. Sokolovskaya, *Mosc. Univ. Chem. Bull.* **29,** 83 (1974).
23. S. V. Popova and V. G. Putro, *Inorg. Mater.* **15,** 947 (1979).
24. L. Pauling, "The Nature of the Chemical Bond," 3rd ed. Cornell Univ. Press, Ithaca, NY, 1948.
25. H. Kleinke, *J. Am. Chem. Soc.* **122,** 853 (2000).
26. C. Röhr, *Z. Naturforsch.* **50b,** 802 (1995).
27. D. E. Sands, D. H. Woods, and W. J. Ramsey, *Acta Crystallogr.* **17,** 986 (1964).
28. H. Kleinke, *Chem. Commun.* (*Cambridge*) 2219 (1998).
29. G. A. Papoian and R. Hoffmann, *Angew. Chem. Int. Ed.* **39,** 2408 (2000).
30. R. Dronskowski and P. Blöchl, *J. Phys. Chem.* **97,** 8617 (1993).
31. T. Hughbanks and R. Hoffmann, *J. Am. Chem. Soc.* **105,** 3528 (1983).